Journal of Visualized Experiments

A robust discovery platform for the identification of novel mediators of melanoma metastasis

--Manuscript Draft--

Article Type:	Invited Methods Collection - JoVE Produced Video
Manuscript Number:	JoVE63186R2
Full Title:	A robust discovery platform for the identification of novel mediators of melanoma metastasis
Corresponding Author:	Eva Hernando, Ph.D. NYU Langone Health New York City, New York UNITED STATES
Corresponding Author's Institution:	NYU Langone Health
Corresponding Author E-Mail:	Eva.Hernando-Monge@nyulangone.org
Order of Authors:	Arman Alberto Sorin Shadaloey
	Alcida Karz
	Eva Hernando
	Rana Moubarak
	Grace Levinson
	Kevin Kleffman
	Orlando Aristizabal
	Youssef Zaim-Wadghiri
	Iman Osman
	Praveen Agrawal
Additional Information:	
Question	**Response**
Please specify the section of the submitted manuscript.	Cancer Research
Please indicate whether this article will be Standard Access or Open Access.	Standard Access ($1400)
Please indicate the **city, state/province, and country** where this article will be **filmed**. Please do not use abbreviations.	New York City/NY
Please confirm that you have read and agree to the terms and conditions of the author license agreement that applies below:	I agree to the Author License Agreement
Please confirm that you have read and agree to the terms and conditions of the video release that applies below:	I agree to the Video Release
Please provide any comments to the journal here.	

TITLE:

A Robust Discovery Platform for the Identification of Novel Mediators of Melanoma Metastasis

AUTHORS AND AFFILIATIONS:

Arman Alberto Sorin Shadaloey[1,2], Alcida Karz[1,2], Rana S. Moubarak[1,2], Praveen Agrawal[1,2], Grace Levinson[1,2], Kevin Kleffman[1,2], Orlando Aristizabal[3,4], Iman Osman[2,5], Youssef Z. Wadghiri[3,4], Eva Hernando[1,2]

[1]Department of Pathology, NYU Grossman School of Medicine, New York, NY 10016, USA
[2]Interdisciplinary Melanoma Cooperative Group, Perlmutter Cancer Center, NYU Langone Health, New York, NY 10016, USA
[3]Department of Radiology, NYU Grossman School of Medicine, New York, NY 10016, USA
[4]Preclinical Imaging Core, NYU Grossman School of Medicine, New York, NY 10016, USA
[5]Ronald Perelman Department of Dermatology, NYU Grossman School of Medicine, New York, NY 10016, USA

Email addresses of co-authors:

Arman Alberto Sorin Shadaloey	(armanalbertosorin.shadaloey@nyulangone.org)
Alcida Karz	(alcida.karz@nyulangone.org)
Rana S. Moubarak	(rana.moubarak@nyulangone.org)
Praveen Agrawal	(Praveen.Agrawal@nyulangone.org)
Grace Levinson	(grace.levinson@nyulangone.org)
Kevin Kleffman	(kevin.kleffman@nyulangone.org)
Orlando Aristizabal	(orlando.aristizabal@nyulangone.org)
Iman Osman	(iman.osman@nyulangone.org)
Youssef Z. Wadghiri	(youssef.zaimwadghiri@nyulangone.org)

Corresponding author:

Eva Hernando	(eva.hernando-monge@nyulangone.org)

SUMMARY:

This article describes a workflow of techniques employed for testing novel candidate mediators of melanoma metastasis and their mechanism(s) of action.

ABSTRACT:

Metastasis is a complex process, requiring cells to overcome barriers that are only incompletely modeled by *in vitro* assays. A systematic workflow was established using robust, reproducible *in vivo* models and standardized methods to identify novel players in melanoma metastasis. This approach allows for data inference at specific experimental stages to precisely characterize a gene's role in metastasis. Models are established by introducing genetically modified melanoma cells via intracardiac, intradermal, or subcutaneous injections into mice, followed by monitoring with serial *in vivo* imaging. Once preestablished endpoints are reached, primary tumors and/or metastases-bearing organs are harvested and processed for various analyses. Tumor cells can be sorted and subjected to any of several 'omics' platforms, including single-cell RNA-seq. Organs

undergo imaging and immunohistopathological analyses to quantify the overall burden of metastases and map their specific anatomic location. This optimized pipeline, including standardized protocols for engraftment, monitoring, tissue harvesting, processing, and analysis, can be adopted for patient-derived, short-term cultures and established human and murine cell lines of various solid cancer types.

INTRODUCTION:

The high mortality associated with metastatic melanoma combined with an increasing incidence of melanoma worldwide[1] (an estimated 7.86% increase by 2025) calls for new treatment approaches. Advances in target discovery hinge upon reproducible models of metastasis, a highly complex process. Throughout the steps of the metastatic cascade, melanoma cells must overcome countless barriers to achieve immune system evasion and colonization of distant tissues[2]. The resilience and adaptability of melanoma cells arise from a multitude of factors, including their high genetic mutational burden[3] and their neural crest origin, which confer crucial phenotypic plasticity[3,4,5]. At each step, transcriptional programs allow metastasizing melanoma cells to switch from one state to another based on cues from crosstalk with the microenvironment, comprising the immune system[6], the extracellular milieu[7,8], and the cellular architecture of physical barriers[9] with which they come in contact. For example, melanoma cells escape immune surveillance by downregulating the expression of important immune-priming tumor-secreted factors[6].

Studies describe a “premetastatic niche,” wherein melanoma cells secrete chemokines and cytokines to prime the distant "target" organ for metastasis[10]. These findings raise important questions about the organ tropism of metastatic melanoma cells and the anatomic route they take to access distant tissues. After intravasation into circulation, melanoma cells are known to metastasize through lymphatics (lymphatic spread) and blood vessels (hematogenous spread)[2,11]. While most patients present with localized disease, a small subset of cases presents with distant metastatic disease and no lymphatic spread (negative lymph node involvement)[11], implying the existence of alternative metastatic pathways for melanoma.

When they colonize a metastatic site, melanoma cells undergo epigenetic and metabolic adaptations[12,13]. To access and invade new compartments, melanoma cells employ proteases[14] and cytoskeletal modifications[11,15], which enable them to traverse to and grow in their new location. The difficulty in targeting melanoma cells resides in the complexity and number of such adaptations; thus, the field should make efforts to recreate experimentally as many steps and adaptations as possible. Despite numerous advances in *in vitro* assays such as organoids and 3D cultures[16,17], these models only incompletely recapitulate the *in vivo* metastatic cascade.

Murine models have shown value by striking a balance between reproducibility, technical feasibility, and simulation of human disease. Intravascularly, orthotopically and heterotopically implanted melanoma cells from patient-derived xenografts or short-term cultures into immune-compromised or humanized mice represent a linchpin of target discovery in metastatic melanoma. However, these systems often lack a crucial biological constraint on metastasis: the immune system. Syngeneic melanoma metastasis models that overcome this constraint are

relatively scarce in the field. These systems, developed in immunocompetent mice, including B16-F10[18], the YUMM family of cell lines[19], SM1[20], D4M3[21], RIM3[22] or more recently, the RMS[23] and M1 (Mel114433), M3 (HCmel1274), M4 (B2905)[24] melanoma cell lines, allow the investigation of the complex role of the host immune response in melanoma progression.

Here, a pipeline for melanoma metastasis target identification is presented. With increasing and larger 'omics' datasets being generated from melanoma patient cohorts, we postulate that studies holding the most clinical promise are those that stem from big data integration, leading to meticulous functional and mechanistic interrogation[25–28]. By using mouse models to study potential targets in the metastatic process, one can account for *in vivo*-specific events and tissue interactions, thus increasing the probability of clinical translation. Multiple methods to quantify metastatic burden are outlined, offering complementary data on the results of any given experiment. A protocol for single-cell isolation from tumors in various organs is described to aid the unbiased characterization of gene expression in metastatic cells, which may precede single-cell or bulk RNA sequencing.

PROTOCOL:

NOTE: The animal procedures involved in the following protocol were approved by the New York University Institutional Animal Care and Use Committee (IACUC). All the procedures are conducted in facilities approved by the Association for Assessment and Accreditation of Laboratory Animal Care International (AAALAC). **Figure 1** depicts the experimental approach.

1. Patient-derived melanoma short-term cultures (STCs)

1.1. Place the tissue in a 60 mm Petri dish with 1 mL of complete RPMI (RPMI 1640 supplemented with 10% fetal bovine serum (FBS), 2 mM L-glutamine, 1 mM sodium pyruvate, 1x MEM non-essential amino acid solution, and penicillin (100 IU/mL)/streptomycin (100 µg/mL)).

NOTE: To enrich the yield of tumor cells, if needed, the tissue surrounding the tumor can be dissected under a microscope in a Petri dish using sterile surgical instruments.

1.2. Finely cut the fresh tissue using sterilized razor blades into 1–2 mm cubes. Add 4 mL of complete RPMI and pipette the contents of the plate up and down 5–10 times with a 10 mL serological pipette.

1.3. Transfer the cell suspension to a 15 mL polypropylene conical tube and spin the cells down (180 × *g* for 5 min at 4 °C). Aspirate the supernatant, resuspend the cell pellet in 1 mL of fresh medium, and transfer the suspension to a 25 cm^2 tissue culture flask.

1.4. To help the remaining tissue fragments attach to the bottom, set the flask tilted at a 20°–30° angle in a tissue culture incubator at 37 °C, 5% CO_2 for 20 min. Lay the flask down flat to allow the medium to cover the tissue, and check the status of the culture daily. Split the cells when they reach 90–100% confluency. Maintain short-term cultures at a "low" passage number.

NOTE: STCs will be established approximately 2 months post cell isolation and culture, although the actual timeline varies between samples and tumor types. After passages 10 to 14, the cell lines will reach 100% purity, containing only melanoma cells[29]. The passage number threshold is empirically determined by observed changes in cell morphology, doubling time, and behavior *in vivo*. To preserve heterogeneity and other characteristics of the parent tumor, do not split more than 1:5.

1.5. Upon establishment of an STC and with any other cell line model to be injected into animals as described in subsequent steps, transduce cells with a reporter.

NOTE: A fluorescent tag (*e.g.*, red fluorescent protein (RFP), green fluorescent protein (GFP)), for example, allows for *ex-vivo* immunofluorescence imaging and sorting of tumor cells by fluorescence-activated cell sorting (FACS). Luciferase enables *in vivo* bioluminescence imaging, a useful tool for monitoring experiments in progress (see section 6).

[**Figure 1**]

[**Figure 2**]

2. Xenograft implantation

NOTE: The experimental procedures described here are conducted in mice that have both adaptive and innate immune systems impaired, NOD.Cg-*Prkdc*^{scid} *Il2rg*^{tm1Wjl}/SzJ (NSG) mice; or mice that lack adaptive immunity, such as the T cell-deficient athymic/nude (NU/J) mice. Animals are of male sex, 8 to 10 weeks of age. Females often exhibit a high incidence of gonadal metastases upon intracardiac injection of tumor cells, which reduces their survival.

2.1. For subcutaneous and intradermal injections, prepare a 1:1 cell suspension by mixing one part of cells suspended in 1x Dulbecco's Phosphate-Buffered Saline (DPBS) with one part thawed extracellular matrix substrate (EMS), and keep on ice at 4 °C. For intravascular (intracardiac, intracarotid, retro-orbital, tail vein, or splenic) injections, suspend the cells in DPBS only.

NOTE: The appropriate volume for intradermal injections should be kept as low as possible (30 µL). For subcutaneous injections, the injected volume can go up to 100 µL, and for intravascular injections, up to 250 µL (based on the weight of the animal). Include in the final cell suspension a 10–30% extra amount of injectate, based on the volume injected and the syringe used to account for the dead volume inside the slip tip and in the needle (e.g., a 1 mL tuberculin syringe with a 30 G, 1 inch needle has a dead volume of 100 µL).

2.2. Conduct a pilot to characterize the behavior of the cell lines in use and the timeline of tumor progression *in vivo*. For intradermal injections, start by injecting 1,000 up to 50,000 cells/30 µL. For subcutaneous injections, start by injecting 10,000 up to 2×10^6 cells/150 µL. For

intravascular (intracardiac, intracarotid, retro-orbital, and splenic) injections, start by injecting 50,000 cells/150 µL.

NOTE: Intravascular injections predispose the animals to embolic events, either by introducing air into the circulatory system or by using a supernumerary number of cells that occlude the small vessels. Mix the cell suspension well to avoid clumping. Prime the syringe before loading the cell suspension. Remove any air bubbles inside the syringe. Keep the cell suspension/syringes on ice until loading and injection time.

2.3. Administer anesthesia by inhalation.

2.4. Set the oxygen level regulator between 1–2 L/min. Place the animal in the induction chamber with the isoflurane vaporizer set at 2.5–5% for induction and 1.5–3% for maintenance.

NOTE: Monitor the breathing and heart rate of the animal while in the anesthesia induction phase. **Do not** leave the animal unattended. **Do not** monitor more than one animal simultaneously. **Titer** the amount of anesthesia to the weight of the animal.

2.5. Move the animal from the induction chamber into the nose cone. Apply sterile petrolatum ophthalmic ointment on the animal's eyes to prevent corneal dryness during the procedure.

2.6. Shave the procedure site with a straight razor blade or scalpel blade tilted at a 30° angle. Clean the skin around the procedure area with 10% povidone-iodine. Before any further steps, assess for a sufficient level of anesthesia by pedal reflex.

2.7. For intradermal injections, perform the entire procedure inside a biosafety cabinet to maintain aseptic conditions.

2.7.1. Anesthetize and shave the animal as described in steps 2.3–2.6.

2.7.2. Grasp and retract the skin backward against the trajectory of the needle stab. Using a 31 G insulin syringe needle, 6 mm long at an acute angle, gently puncture the skin with the bevel facing upward.

2.7.3. Feel the pressure release at the tip of the needle. Advance gently to stay inside the intradermal compartment and not pass through the entire skin depth into the subcutis. **Crucial:** If one slips into the subcutaneous space, remove the needle, change the injection area and reinsert the needle. Inject the entire volume (30 µL) of cell suspension slowly until a dome-shaped wheal is observed.

NOTE: Low injection volumes will induce less dissection of the skin layers and less architectural distortion.

2.7.4. Keep the needle in and count to 5.

NOTE: EMS becomes viscous at body temperature, helping to avoid backflow through the needle puncture wound.

2.7.5. Remove the needle and single-house the animal in a cage on a warm pad to recover. Return the animal to the vivarium cage after regaining consciousness when it is sternal and ambulatory.

NOTE: Monitor the animal continuously during all the procedures described in this protocol. **Do not** leave the animal unattended or monitor more than one animal simultaneously.

2.7.6. Monitor the progression of tumor growth, weight loss, and overall health status 2 times per week in the initial growth phase and 3 times per week after animals start losing weight. During these monitoring sessions:

2.7.6.1. Take measurements with calipers and use the length (L) and the width (W) dimensions of the tumor to calculate the volume (V) with the formula:

$$V = (W2 \times L)/2$$

2.7.6.2. Weigh the animals and plot a chart to monitor their weight loss. Monitor the animal for signs of tumor ulceration, neurological, locomotor, and/or behavioral signs (lethargy, lack of grooming, low food or water intake).

NOTE: Euthanize the animals immediately after observing signs of advanced disease (more than 20% weight loss, a body condition score of <2, extremely reduced activity levels, paralysis, or seizures). Use the euthanasia method approved by the institution's IACUC (e.g., an automated tabletop CO_2 chamber is used to expose the animals to CO_2 for 15 min followed by a secondary method of euthanasia, either cervical dislocation, decapitation, or pneumothorax induced bilaterally by incising the ribcage).

2.8. For subcutaneous injections:

2.8.1. Perform the entire procedure inside a biosafety cabinet to maintain aseptic conditions.

2.8.2. Anesthetize and shave the animal as described in steps 2.3–2.6.

2.8.3. Using a 28 G to 31 G insulin syringe needle, 6 mm in length at an acute angle, gently puncture the skin with the bevel facing upward. Feel the pressure release at the tip of the needle **twice** while passing through the epidermis, dermis, and hypodermis.

NOTE: The second time a pressure release is felt at the tip of the needle indicates the subcutaneous compartment has been reached.

2.8.4. Inject the entire volume (30–100 µL) of cell suspension slowly until an elongated ellipse-shaped wheal is observed. Keep the needle in and count to 5. Count to 10 for larger volumes (more than 50 µL).

NOTE: EMS becomes viscous at body temperature, helping to avoid backflow through the needle puncture wound.

2.8.5. Remove the needle and single-house the animal in a cage on a warm pad to recover. Return the animal to its vivarium cage after regaining consciousness when it is sternal and ambulatory.

NOTE: During the postprocedure monitoring, observe for any signs of complications (low respiratory rate, bleeding, slow recovery) and address them appropriately. If no improvement is observed, proceed to humane euthanasia procedures described in the NOTE of step 2.7.6.2.

2.8.6. Monitor the animal for tumor growth, weight loss, and overall health status as described in point 2.11.9.

2.9. For intracardiac injections:

2.9.1. Perform the entire procedure inside a biosafety cabinet to maintain aseptic conditions.

2.9.2. Anesthetize as described in steps 2.3–2.5.

2.9.3. Transfer the animal onto the heated platform of the ultrasound machine and secure the mouse with hypoallergenic tape to the nose cone.

2.9.4. Shave the thorax with a straight razor blade or scalpel blade tilted at a 30° angle. Clean the skin around the procedure area with 10% povidone-iodine.

2.9.5. Before any further steps, assess for a sufficient level of anesthesia by pedal reflex. Apply ultrasound gel on the procedure site.

2.9.6. Capture the cardiac window with the ultrasound probe. Position the ultrasound probe in the middle of the thorax on the left side of the animal to capture a horizontal window oriented to obtain a cross-sectional view (short axis) of the left ventricle. Ensuring that the long axis of the probe faces upwards, fix the probe at a 50° angle and the heated platform at a 20° angle. Lock the probe and the support frame in position.

2.9.7. Draw up the cell suspension while working inside the safety cabinet in a tuberculin 1 mL syringe with a 30 G, 1 inch needle. Remove any air bubbles present in the syringe.

NOTE: It is important to create and maintain a single-cell suspension as cells are processed and later injected. Removing air bubbles is an important step to avoid air embolism. A well-primed syringe-needle system will prevent unnecessary, avoidable deaths in the experimental group. Always draw more volume into the syringe than will be injected. The extra volume will help remove the air by injecting back into a 1.5 mL tube some of the cell suspension.

2.9.8. Lock the syringe in the stereotactic injector. Under ultrasound guidance, advance the needle through the thoracic wall into the left ventricle of the heart. Inject the entire volume (100–250 µL) of cell suspension slowly.

2.9.9. Remove the needle and single-house the animal in a cage on a warm pad to recover. Return the animal to its vivarium cage after regaining consciousness when it is sternal and ambulatory. Monitor the animal for tumor growth, weight loss, and overall health status as described in step 2.7.6.

2.10. For intracarotid injections:

2.10.1. Perform the entire procedure on a properly disinfected surface to help maintain aseptic conditions.

2.10.2. Anesthetize the animal with a ketamine (100 mg/kg) and xylazine (10 mg/kg) cocktail by intraperitoneal injection with an insulin syringe, 28 G needle. Apply sterile petrolatum ophthalmic ointment on the animal's eyes to prevent corneal dryness during the procedure.

2.10.3. Shave the procedure area with a straight razor blade or scalpel blade tilted at a 30° angle. Before any further steps, assess for a sufficient level of anesthesia by pedal reflex.

2.10.4. Place the animal under a stereo microscope on a warming pad. Clean the skin around the procedure area with 10% povidone-iodine.

2.10.5. Don sterile personal protection equipment (PPE) and sterile gloves. Prepare the sterile field by laying a sterile drape over the animal's body.

NOTE: If the sterile drape does not have a hole appropriate for the size and location of the incision, fold the drape in half and use Metzenbaum scissors to cut the appropriate size hole in the middle of the sterile drape.

2.10.6. Use a scalpel or Iris scissors to incise the skin from half the neck down to the sternum. With two microsurgery forceps, bluntly dissect apart the 2 submandibular salivary glands in the midline plane. Use an electric cautery for hemostasis, if necessary.

2.10.7. Dissect the fascia surrounding the common carotid artery (CCA) from the manubrium towards the bifurcation and continue medially to free up the posterior wall of the external carotid. Clip the external carotid artery (ECA) temporarily before injecting.

NOTE: When dissecting around the circumference of the CCA, care has to be taken not to damage the vagus nerve (lies lateral to the artery).

2.10.8. Load the cell suspension in an insulin syringe with a 31 G, 6 mm needle.

2.10.9. Pass two 7-0 ligatures under the CCA, and perform a loose instrument knot for each of the two ligatures. Use a 5 mm, 10 G pressure vessel clip and temporarily clip the ECA. Tie the proximal ligature; then, tie the distal ligature loosely (next to the bifurcation of the CCA). Use the distal loop later to control the bleeding post injection.

2.10.10. Using an insulin syringe with a 31 G, 6 mm needle, gently puncture the CCA with the bevel of the needle facing upward and at an acute angle. Inject the entire volume (50–150 µL) of cell suspension slowly.

2.10.11. Grip the distal loop with the forceps and lift it while removing the needle to occlude the lumen of the CCA and stop the bleeding. Exchange the syringe with a #7 Jewelers forceps and tie down the distal loop.

2.10.12. Throw another instrument knot on the distal ligature and remove the vessel clip off the ECA. Control the surgical field for bleeding and cauterize any bleeding vessels before closure. Use a 9 mm stapling device to close the skin of the animal and place the animal on a warm pad to recover.

NOTE: Remove the staples 7–10 days post-surgery.

2.10.13. Administer analgesic medication subcutaneously–Buprenorphine (0.3 mg/mL) every 24 h for 72 h post-surgery at a concentration of 0.1 mg/kg.

NOTE: Alternatively, consider using an extended-release analgesic medication, which requires 1 dose every 72 h.

2.10.14. Return the animal to its vivarium cage after regaining consciousness when it is sternal and ambulatory. Monitor the animals postoperatively daily for signs of surgical site infection or pain, general health status, and complications.

NOTE: Animals that do not recover well from survival surgery may be given additional doses of pain medication and euthanized humanely if not fully recovered by 72 h post-surgery.

2.10.15. Monitor the animal for tumor growth, weight loss, and overall health status as described in step 2.7.6.

2.11. For retro-orbital injections:

NOTE: Use this technique as an alternative to tail vein injections when the operator is trained and proficient in this technique and when there is a strong scientific justification. Cell suspensions delivered via this route can induce tumor growth in the retro-orbital space; hence, careful consideration should be given to the risks and benefits when choosing this technique. For example, to take advantage of the direct circulatory connection of the retro-orbital venous sinus with the intracerebral veins via anastomoses, select this method when brain tumor formation has failed using other injection routes.

2.11.1. Perform the entire procedure inside a safety cabinet to maintain aseptic conditions. Don sterile PPE and gloves.

2.11.2. Anesthetize the animal as described in steps 2.3–2.5.

NOTE: For this procedure, do not apply sterile petrolatum ophthalmic ointment to the animal's eyes because this will impede injection; apply only local anesthetic drops.

2.11.3. Load the cell suspension in an insulin syringe with a 28–31 G, 6 mm needle.

2.11.4. With the animal in a prone position, retract the eyelids until the eye protrudes. Apply 1 droplet of local anesthetic into the eye on the side undergoing the procedure.

2.11.5. Insert the needle at a 30–45° angle between the eye and the medial epicanthus with the bevel facing downwards. Inject the cell suspension (10–150 µL) slowly.

NOTE: Slower movements prevent damage to the eye and the backflow of the injectate.

2.11.6. Perform the steps described in 2.7.5–2.7.6.

2.12. For splenic injections:

2.12.1. Perform the entire procedure inside a safety cabinet to maintain aseptic conditions. Don sterile PPE and sterile gloves.

2.12.2. Anesthetize and shave the animal as described in steps 2.3–2.6.

2.12.3. Place the animal in a right lateral recumbent position. Prepare the surgical field as described in steps 2.10.4 (povidone-iodine)–2.10.5.

2.12.4. Using Metzenbaum scissors or a scalpel, make a 1 cm incision in the left flank in the abdominal wall followed by an incision into the peritoneum.

NOTE: The spleen will be seen through the translucent abdominal wall after making an incision in the skin. Perform the peritoneal incision exactly on this site.

2.12.5. Expose the spleen and the splenic hilum through the incision. Using a 28–31 G insulin syringe needle, 6 mm in length, gently puncture the spleen with the bevel of the needle facing upward and at an acute angle.

NOTE: If the puncture wound bleeds, cauterize the site to limit bleeding and backflow.

2.12.6. Inject the entire volume (50–100 µL) of cell suspension slowly. Remove the needle. Place a small gauze on the spleen and apply pressure with forceps. Clamp the spleen lightly between the gauze using fine mosquito forceps and wait for 15 min.

2.12.7. Perform a splenectomy by tying the splenic hilum with a 3-0 or 4-0 silk suture, cauterizing the vessels if necessary. Close the peritoneum with a 5-0 polydioxanone (PDS) or polyglycolic acid absorbable suture.

2.12.8. Perform the steps described in steps 2.7.5–2.7.6.

NOTE: Animals that present bleeding complications or that have not recovered fully post surgery should be humanely euthanized. Remember that the wellbeing of the mice is the priority at all times.

3. Staged survival surgery (SSS)

3.1. Based on the experimental conclusions from step 2.2, determine the proper time to survival surgery. Depending on the cell line and experimental hypothesis, select an earlier time point for tumor resection (at a tumor volume = 150 mm^3) or a later time point (at a tumor volume = 500 mm^3).

NOTE: The tumor volume limit is 1,500 mm^3 when the tumor burden is high enough to be detrimental to the wellbeing of the animal and predisposes to complications.

3.2. Anesthetize and shave the animal as described in steps 2.3–2.6.

NOTE: The entire procedure is performed inside a biosafety cabinet.

3.3. Prepare the surgical field as described in steps 2.10.4 (povidone-iodine)–2.10.5.

3.4. Using Iris scissors or a scalpel, incise the skin, maintaining a 5–7 mm resection margin from the edge of the tumor.

NOTE: The margin for resection depends on the ability of the tumor to spread locally. For aggressive tumors, increase the resection margin while making sure enough skin is left to perform the wound closure.

3.5. In the case of intradermal tumors, resect the tumor along with the circumferential skin.

3.6. For subcutaneous tumors, dissect and remove the tumor under the skin.

NOTE: If the tumor invades the peritoneum and/or the skin, resect it *en bloc* with the tumor and close the peritoneum with 5-0/4-0 PDS or polyglycolic acid absorbable sutures.

3.7. Close the wound with the 9 mm stapling device.

NOTE: Staples are removed 7–10 days post surgery. Animals with bleeding complications or that have not regained full consciousness post surgery should be humanely euthanized. Administer analgesic medication and place the animal on a warm pad to recover. Continue administering analgesic medication for 72 h post surgery, once every 24 h according to step 2.10.13.

3.8. Single-house the animal in a cage, on a warm pad, to recover. Return the animal to the vivarium cage after regaining consciousness when it is sternal and ambulatory.

3.9. Continue to monitor the animal post surgery for local recurrences, weight loss, and overall health status according to step 2.7.6.

4. *In vivo* imaging (Figure 2A)

4.1. Administer D-luciferin substrate (150 mg/kg) to animals by intraperitoneal injection with a 1 mL insulin syringe, 28 G needle.

NOTE: Tumor cells must be stably transduced with the luciferase cDNA.

4.2. Induce anesthesia as described in steps 2.3–2.5, 6 min after the D-luciferin substrate injection.

4.3. Perform imaging using a bioluminescence imaging (BLI) scanner (*in vivo* imaging system).

4.4. Move the animal inside the imaging chamber and into the nose cone. Image up to 5 animals simultaneously, depending on the imaging system's capacity.

4.5. Start the instrument by pressing **initialize**. Set the exposure time setting to **auto** (1–120 s).

4.6. Capture a blank image to subtract any background if needed. Click **acquire** and save the image after the acquisition sequence is completed.

4.7. Place the animal back in a cage, which sits with 50% of the surface area of the base over a warming pad to recover from anesthesia. Return the animal to the vivarium cage after regaining consciousness when it is sternal and ambulatory.

4.8. For data analysis in the same *in vivo* imaging software with which the images were captured, navigate to the folder where the images are saved, and open the images of all the mice pertaining to the experiment at once.

NOTE: Analysis of one image at a time will not allow normalization across groups.

4.9. Set the units to **radiance** (not **counts**). Ensure that the checkbox indicating **Individual** is **NOT** checked, as this will preclude normalization of signal across groups.

4.10. Using the **Region of Interest (ROI)** drawing tool, draw circular ROIs for the brain region and rectangular ROIs for the body. Be careful to exclude the ears and nose in the brain ROI, as they tend to emit unspecific luminescence. To minimize bias in this process, draw ROIs on the photographs of the mice only, without the luminescent signal overlaid.

4.11. Select **Measure ROIs** to quantify the signal and export the data to a spreadsheet. Analyze differences between groups by plotting total luminescent flux (p/sec/cm^2/sr) in body regions of interest.

NOTE: To assess differences between groups in brain tropism specifically, calculate the ratio between the brain signal and body signal for each mouse. This controls for intermouse variation in overall tumor burden and differences in levels of luciferase expression between experimental groups.

5. *Ex vivo* magnetic resonance imaging

5.1. Perform *ex vivo* MRI immediately after euthanasia. Alternatively, harvest the organs of interest, fix them in formalin for up to 72 h, and perform the imaging at a later timepoint.

5.2. Acquire the images with a 7-Tesla (7-T) (300-MHz) micro-MRI system equipped with an NMR console and a zero-boil-off, horizontal bore magnet or similar equipment.

NOTE: The need for an actively shielded gradient coil insert with the correct trade-off of performance is crucial. It must provide gradient linearity of at least 50 mm of dynamic spherical volume (DSV) to cover the set of samples examined simultaneously with no geometric distortion. The combination of gradient strength (ranging from 440 to 750 mT/m) and duty cycle enabling maximum simultaneous DC currents ranging from 3 x 30 A to 3 x 87 A will enable adequate imaging performance. The gradient coil insert used (see the **Table of Materials**) enables the following performance: 660 mT/m, 130 µs rise time, 3 x 87 A, and a DSV = 80 mm.

5.3. Perform the scans with a commercial transmit-receive circularly polarized whole mouse body radiofrequency coil (OD = 59 mm, ID = 38mm, L = 40 mm) tuned to 300.16 MHz, the ^{1}H proton Larmor frequency.

NOTE: This rf probe enables the acquisition of 3D datasets with submillimetric isotropic resolution (<150 µm) during overnight scans spanning 8–12 h.

5.4. Detect the tumor burden using multiple sequences[30].

NOTE: Hyperintense signal detected by a T_2-weighted, Rapid Imaging with Refocused Echoes (RARE) sequence recognizes edema surrounding tumors.

5.5. Perform the 3D RARE sequence with the following acquisition parameters: $[120\ \mu m]^3$ isotropic resolution; acquisition time 5 h, 27 min; repetition time TR = 500 ms; echo spacing ES = 12.7 min; Turbo factor TFx = 12; effective echo time TE_{eff} = 76.2 ms; bandwidth BW = 75 KHz; Matrix size = 284^3; field of view (FOV) = $[4.0\ mm]^3$; number of averages Nav = 6.

5.6. Detect metastases using the following parameters.

5.6.1. For pigmented metastases with signal brightening, use a T_1-weighted 3D Gradient echo sequence with the following parameters: $[120\ \mu m]^3$ isotropic resolution; acquisition time 2 h, 41 min; repetition time TR = 20 ms; echo time TE = 4.0 ms; flip angle FA = 18°; bandwidth BW = 75 KHz; Matrix size = 2843; FOV = $[34.0\ mm]^3$; number of averages Nav = 6.

5.6.2. For unpigmented and/or hemorrhagic metastases, use a hypointense signal when acquiring under a T_2*-weighted, multigradient echo (MGE) sequence (3D MGE, $[120\ \mu m]^3$ isotropic resolution; acquisition time 3 h, 35 min; repetition time TR = 40 ms; echo time TE = 3.6 ms; echo spacing ES = 3.2 ms; 4 echoes; flip angle FA = 20°; bandwidth BW = 100 kHz; Matrix size = 284^3; FOV = $(34.0\ mm)^3$; number of averages Nav = 4.

5.7. Use all 3 sequences to quantify tumor burden.

5.8. Crossreference the tumor areas identified during analysis with histological sections to ensure accuracy. See sections 7 and 8.

6. Tissue processing for single-cell or bulk RNA sequencing

6.1. For euthanasia, anesthetize the animal with an overdose of ketamine (300 mg/kg) and xylazine (30 mg/kg) cocktail by intraperitoneal injection with an insulin syringe, 28 G needle. Wait for 5 min and check the level of anesthesia by pedal reflex.

NOTE: The animal will present an agonal pattern of breathing, which indicates the progression of diaphragmatic paralysis. Animals can be euthanized using alternative techniques.

6.2. Perform a secondary method of euthanasia, either by cervical dislocation, decapitation, or pneumothorax induced bilaterally by incising the ribcage.

6.3. Dissect the organs of interest and place them on a plate (12-well) containing Hank's buffered Salt Solution (HBSS) on ice. Work expeditiously and keep the tissue on ice at all times to maximize cell viability.

6.4. Prepare a 6-well plate with 3 mL of HBSS in each well.

6.5. To visualize and further help guide the dissection, use a fluorescence microscope and identify the labeled areas.

6.6. Dissect the fluorescent areas and place the tissue fragments in the 6-well plate (1 fragment per well if individual metastatic foci are to be analyzed or multiple fragments from one organ if multiple metastases in the same organ are to be analyzed). Use sterile razor blades to mince the tissue into fragments as small as possible (without spending more than 1–2 min on this step for each sample).

NOTE: Limiting the processing time of the tumors helps preserve cell viability.

6.7. Aspirate and transfer the contents of each well to a 15 mL conical tube.

NOTE: Cut the tip of a 1,000 µL pipette tip to facilitate the transfer of larger fragments.

6.8. Add 1 mL of HBSS to the well and ensure that the remaining tissue fragments/cells are transferred to the 15 mL tube, which will contain a final volume of 4 mL. Add 50 µL of collagenase type I (40 mg/mL) and 12.5 µL DNase I (2,000 units/mL) to each tube.

6.9. Place the conical tubes in a water bath heated at 37 °C for 45 min. Briefly vortex the conical tubes every 5 min.

6.10. Prewet a 70 µm strainer with HBSS. Use the capped end of a sterilized microcentrifuge tube or the plastic part of a syringe plunger and grind the tissue homogenates through a 70 µm strainer into a new 50 mL conical tube.

NOTE: Prewetting the strainers with HBSS or FACS buffer facilitates straining.

6.11. Wash the strainer with 1 mL of HBSS. Prewet a 40 µm strainer with HBSS. Filter each sample again through a 40µm strainer into a new 50 mL conical tube. Add 1 mL of FBS to the 40 µm strainer to wash it. Keep the conical tubes on ice all the time.

6.12. Fill up the conical tube to 50 mL with ice-cold DPBS. Spin down the cells (180 × *g* for 10 min at 4 °C). Discard the supernatant, being careful not to lose the cell pellet.

NOTE: For **brain samples**, resuspend the cells in 2.5 mL of 38% density separation solution (dilute in HBSS and store at room temperature (RT)). Transfer to 5 mL FACS tubes. Spin for 20 min at 800 × *g*. Cut the tip of A 1,000 µL pipette tip and remove the top fat layer. Do not leave any fat on the

walls of the tubes. If any fat is left, spin down again and repeat the process. This is a **critical** step. Remove the rest of the liquid phase (the pellet will be translucent and hard to visualize).

6.13. Resuspend the cells in 1 mL of red blood cell (RBC) lysis buffer and incubate for 60 s at RT. Quench the lysis solution by adding 20 mL of DPBS.

6.14. Spin down the cells at 180 × *g* for 10 min at 4 °C. Remove the supernatant and resuspend the cells in 2 mL of FACS buffer (5% FBS in DPBS) for sorting labeled cells.

6.15. Proceed with sorting and/or library preparation for either bulk or single-cell RNA-sequencing.

NOTE: Cells can be spun down, snap-frozen, and stored at -80 °C prior to RNA isolation for bulk RNA-seq.

7. Mouse tissue perfusion and preparation for immunohistological analyses

7.1. Anesthetize the animal with an overdose of ketamine (300 mg/kg) and xylazine (30 mg/kg) cocktail by intraperitoneal injection with an insulin syringe and a 28 G needle.

7.2. Expose the heart by gross dissection and make an incision in the right atrium. Hold the heart gently in place with long, curved forceps facing anteriorly.

NOTE: Formalin and paraformaldehyde (PFA) are carcinogens. Read the Safety Data Sheet (SDS), avoid exposure to fumes, and wear the appropriate PPE.

7.3. Using a 10 mL syringe with a 22 G, 22 mm needle, inject 10 mL of DPBS followed by 10 mL of 4% PFA into the left ventricle.

7.4. Proceed to harvest the organs and load them into prelabeled histological cassettes. Place the cassettes in an appropriately sized container that accommodates enough fixative (formalin) to cover the tissues.

NOTE: Ideally, the fixative volume should be 5–10 times the volume of the tissues.

7.5. Fix the organs inside the histological cassettes in 10% formalin for 48–72 h. Discard the 10% formalin and wash the cassettes twice with 1x DPBS.

7.6. Begin the dehydration process by immersing the cassettes in 70% ethanol for 2 h. Continue to immerse the cassettes successively in increasing ethanol concentrations: 80%, 95%, 100% for 1 h each. Change the 100% solution twice after 1.5 h. Immerse the cassettes in xylene for 1.5 h and perform three changes of the solution.

7.7. Embed the cassettes in paraffin wax at 58–60 °C. Section the paraffin blocks. Proceed to hematoxylin and eosin (H&E) or immunohistochemistry staining.

7.8. To identify melanoma cells, use either of these markers or a panel: S100, Melan-A, HMB-45, Tyrosinase, MITF. When possible, use Nuclear Mitotic Apparatus Protein (NuMA) staining as it is a highly specific human cell marker.

NOTE: NuMA staining offers a sharp delineation between host (mouse) and engrafted cells (human) that aids in image processing and subsequent tumor quantification stages.

8. Nuclear Mitotic Apparatus Protein (NuMA) staining (Figure 3)

8.1. Use an anti-NuMA antibody as a highly human-specific mitotic spindle marker for the identification and quantification of metastatic burden in tissue sections.

NOTE: Due to the specificity of the antibody in xenografts, highly specific and sensitive identification of melanoma cells is achieved.

8.2. If chromogenic immunohistochemistry for NuMA is performed on an automatic immunostaining instrument, follow these steps as described[31]:

8.2.1. Deparaffinize the sections in xylene and rehydrate them in sequentially decreasing ethanol concentrations. Keep the slides submerged for 15 min in xylene and transfer them to 100% ethanol for another 15 min.

NOTE: The remainder of the ethanol rehydration steps (95%, 80%, 75%) will last for 3 to 5 min each.

8.3. Rinse the slides in deionized water.

8.4. Perform epitope retrieval by submerging the slides in a container (e.g., Coplin staining jar) in 10 mM sodium citrate buffer, pH 6.0, in a 1200 Watt microwave oven at 100% power for 10 min.

8.5. Use unconjugated, polyclonal rabbit anti-human NuMA antibody for labeling, diluted 1:7,000 in Tris–bovine serum albumin (BSA) (25 mM Tris, 15 mM NaCl, 1% BSA, pH 7.2). Run the appropriate positive and negative controls in parallel with the study sections.

8.6. Incubate the slides with the primary antibody for 12 h. Detect the primary antibody with goat anti-rabbit HRP conjugated multimer and visualize the complex with 3,3-diaminobenzidine and a copper sulfate enhancer.

8.7. Wash the slides in distilled water, counterstain with hematoxylin, dehydrate, and mount with permanent medium.

NOTE: The dehydration steps are the reverse of the rehydration steps described above. Scan the slides with the available scanner at 20x or 40x and upload them to a database.

8.8. Using software, draw regions of interest to include all NuMA-stained cells within the organ tissue, excluding other organ parenchyma and empty spaces.

8.9. Adjust the settings to categorize the NuMA-positive and NuMA-negative cells while using appropriate positive and negative controls for each organ. Use an established software algorithm to quantify the total number/percentage of NuMA-positive cells for each sample.

9. Tissue slice immunofluorescence

NOTE: To identify the metastatic stage in which a particular gene candidate is required (e.g., extravasation vs. survival after seeding), one can determine tissue slice immunofluorescence at different time points to track tumor cell progression from injection to distant organ invasion, seeding, and growth. This approach allows the addition of markers for neighboring cells to capture the extravasation event and the surrounding tumor microenvironment changes.

9.1. Perfuse the animal as described in steps 7.1–7.3. Harvest the organs of interest and transfer them into prelabeled containers filled with 4% PFA. Fix the tissue for 24 to 48 h. Section the tissue using a vibratome into 30–50 µm thick slices.

NOTE: Thickness should be optimized. Slices between 30 µm and 50 µm thickness are recommended, especially when performing z-stack imaging.

9.2. Incubate the slices in blocking buffer (10% Normal Goat Serum, 2% BSA, 0.25% Triton X-100 in DPBS) for 2 h at RT.

9.3. Perform an optimization staining experiment.

NOTE: As antigen retrieval time, buffers used for antigen retrieval, temperature, antibodies/different lots, and the type of tissue influence the staining, optimization experiments are necessary.

9.4. Add primary antibodies and incubate for an optimized time, temperature, and at an optimized dilution (**Table 1**).

NOTE: Use appropriate controls of primary, secondary, and unstained tissue samples.

9.5. Wash the slices 3 times for 5 min in 0.25% Triton X-100 in DPBS.

9.6. Incubate the slices in secondary antibody diluted in blocking solution for the desired time (**Table 1**).

9.7. Wash the slices 3 times for 5 min in 0.25% Triton X-100 in DPBS.

9.8. Stain the nuclei with 4',6-diamidino-2-phenylindole [DAPI] diluted 1:1,000 in DPBS or blocking buffer for 5 min.

9.9. Place the tissue slices on glass slides. Add 2 drops of antifade fluorescence mounting medium to a coverslip and mount it onto glass slides, making sure the slices are fully covered by mounting medium.

NOTE: Ensure there are no air bubbles directly on the slices as this distorts microscopy.

9.10. Capture confocal images with the available microscope using a 60x oil immersion objective.

NOTE: Make sure all the images are scanned with the same Airy Unit setting.

9.11. Capture non-confocal images using the microscope at 10x, 20x, or 40x.

NOTE: When acquiring confocal images, apply the same settings parameters (voltage, airy units, and gain) across all the images within the experiment

9.12. Upload the pictures in an image analysis software and analyze them comparing the parameters of choice (i.e., area, number, intensity of markers, or contact with adjacent cells).

REPRESENTATIVE RESULTS:

The following figures illustrate how the described workflow has been applied for the identification of novel metastasis drivers of melanoma. **Figure 2** summarizes the results of a published study in which the effects of silencing the fucosyltransferase FUT8 in *in vivo* melanoma metastasis were studied[40]. Briefly, analysis of human patient glycomic data (obtained by lectin arrays) and transcriptomic profiling revealed increased levels of alpha-1,6-fucose associated with progression from primary to metastatic melanoma, consistent with an increase in the corresponding fucosyltransferase (FUT8).

113/6-4L melanoma cells transduced with lentiviruses carrying an FUT8 shRNA or the corresponding non-targeting control (shNTC) were introduced by ultrasound-guided intracardiac injection into immunodeficient mice (NSG), as described above (protocol section 2). The mice were monitored for metastatic dissemination by *in vivo* BLI. The mice were euthanized at the end of the experiment (protocol section 7), and the organs were examined for *ex vivo* fluorescence and processed for histological analyses. In addition to H&E, NuMA staining was performed to specifically identify human cells in murine tissues. As illustrated in **Figure 3**, NuMA-stained sections were processed by digital imaging to quantify the metastatic burden across multiple sections and experimental groups. A similar workflow can be applied to assess the contribution of other candidate genes to melanoma metastasis.

FIGURE AND TABLE LEGENDS:

Figure 1: Schematic illustrating the described workflow, from patient data integration to generation and analysis of *in vivo* data from mice. Abbreviations: LOF = loss of function; GOF = gain of function.

Figure 2: Examples of BLI, brightfield, *ex vivo* fluorescence, and H&E staining images illustrating the multipronged approach for the analysis of candidate genes' effects on melanoma metastasis. (**A**) BLI , (**B**) brightfield, (**C**) *ex vivo* fluorescence, and (**D**) H&E staining images. The images used for the purpose of illustration correspond to an experiment in which 131/6-4L melanoma cells transduced with a non-targeting control shRNA (shNTC) or an shRNA targeting FUT8 were injected into immunodeficient (NSG) mice. FUT8 silencing impaired the metastatic dissemination of melanoma cells. Scale bars and color bar = p/sec/cm^2/sr × 10^6 (**A**), 100 mm (**B**, **C**), 100 µm (**D**). Abbreviations: BLI = bioluminescence imaging; H&E = hematoxylin and eosin; shRNA = short hairpin RNA; shNTC = non-targeting control shRNA; NSG = non-obese diabetic severe combined immunodeficiency gamma; FUT8 = fucosyltransferase; BF = brightfield; RFP = red fluorescent protein.

Figure 3: NuMA-stained lung sections. (**A**) *Left,* representative images of NuMA-stained lung sections from Group I (melanoma cells infected with control lentivirus) and Group II (melanoma cells infected with a metastasis suppressor-expressing lentivirus). Scale bars = 1,000 µm. Insets display metastatic foci (middle) that can be quantified using software. *Right*, metastatic melanoma cells are labeled green, and the organ area is delimitated by a green hatched line. NuMA-negative cells are labeled in blue. Scale bars = 100 µm. (**B**) Example of a micrometastasis in NuMA-stained lung sections illustrates the sensitivity of the software in detecting a small number of cells. Scale bars = 100 µm. Abbreviation: NuMA = Nuclear Mitotic Apparatus Protein.

Table 1: Antibody and incubation conditions for brain slice immunofluorescence.

Table 2: Breakdown of results from representative *in vivo* experiments of various human melanoma cell lines and short-term cultures following the described protocol.

DISCUSSION:

The aim of this technical report is to offer a standardized, top-to-bottom workflow for the investigation of potential actors in melanoma metastasis. As *in vivo* experiments can be costly and time-consuming, strategies to maximize efficiency and increase the value of the information obtained are paramount. One important aspect to consider is the expected incidence of observed brain metastases. We observed an incidence of 80 to 100% brain parenchyma penetrance in these models. Thus, in knockdown experiments, group sample sizes of 10 versus 10 achieve 80% power to detect a difference of 1.3 between the null hypothesis that both group means are equal and the alternative hypothesis that the mean of group 2 (prometastasis) is 1.3 SD, with a common group SD 1.0 and with a significance level (alpha) of 0.05 when using a two-sided two-sample *t*-test. When the model is 100% penetrant, groups of 10–12 animals allow statistically significant

differences to be observed if the effect is observed in more than 25% of the animals. A two-sided log-rank test with an overall sample size of 20 subjects (10 subjects in each arm) achieves 80.0% power at a 0.05 significance level to detect a hazard ratio of 0.2251 when the control group hazard rate is a hazard ratio of 1.0.

It is imperative to use complementary approaches throughout to crossvalidate findings within the same experiment. For example, both NuMA immunohistochemical staining and BLI are complementary methods of quantitating metastatic burden because neither is comprehensive. While BLI is an invaluable, noninvasive method of tracking tumor progression *in vivo*, these data are inherently of low resolution.

NuMA staining allows for meticulous analysis of metastatic burden in fixed organs; however, comprehensive sectioning through the entire tissue thickness is impractical. As such, only a sample of each organ can be stained. Indeed, in the experience of the authors, BLI results are not always directly proportional to the tumor burden evident in histopathological analysis. This is in part due to the limited sensitivity of this method, particularly in the brain, because of transcranial attenuation[32]. In addition, these data can be affected by incomplete luciferin uptake and/or variable luciferase expression. Therefore, BLI should be interpreted in conjunction with *ex vivo* imaging and histopathologic studies.

Histological evaluation of tissue samples treated with generic stains, such as H&E, demands specialized anatomopathology training, is often low-throughput, and is prone to interobserver variations. The authors are currently working with bioinformatics colleagues to standardize and accelerate experimental data analysis to develop a machine learning algorithm for automated and reliable quantitation of metastatic burden as a percentage of organ tissue section in histopathologic images. These and other tools will be critical for the field, especially as the role of the metastatic microenvironment comes into focus at a finer resolution (e.g., spatial transcriptomics). Nevertheless, expert histopathological evaluation of the tissue is essential, particularly in subtypes of brain metastasis such as leptomeningeal, a biologically distinct subtype, which is easily misinterpreted as parenchymal brain metastasis via BLI alone. NuMA staining (protocol section 8) accelerates the histopathologic assessment of metastatic burden, allowing for unbiased identification and quantitation of human cells in mouse organs. However, distinction between anatomic compartments on NuMA-stained sections, such as the brain parenchyma versus the leptomeninges, is critical to gain further biological insights.

The techniques described herein may be used to investigate the functional relevance of genes of interest to the melanoma metastatic cascade. It is critical to select a model with a reproducible phenotype that is appropriate for the study in question. For example, a gene upregulated in human patient samples of metastasis can be “knocked down” to assess if it decreases metastatic burden compared to a control group. This approach is best carried out in a model cell line or short-term culture that features both a) high expression of the gene of interest and b) generates significant metastatic burden with reliable kinetics when injected into mice, such that a decrease in metastatic capacity will be appreciable and assignable to the genetic perturbation being tested.

Also crucial in experimental design is the selected mode of injection most appropriate to the stage of metastasis under investigation. Each stage of the metastatic cascade presents distinct biological and physical barriers to melanoma cells; these pathways are modeled better by some methods compared to others. Investigators seeking to answer questions on the initial stages of metastasis, namely invasion and intravasation, should employ the techniques outlined in protocol section 2 for intradermal and subcutaneous injections, respectively, followed by survival surgery (protocol section 3). Importantly, these procedures mimic the process by which primary melanomas are resected in humans, after which a patient may or may not present with metastasis. While technically more delicate than subcutaneous injection, the intradermal route plants tumor cells in the anatomic compartment where melanomas develop in human patients. This is particularly important in studies of immune surveillance of melanoma, as the skin has a unique ecosystem of patrolling immune populations[33].

However, if the hypothesis being tested centers on later stages of metastasis, such as extravasation from the arterial circulation, methods such as intracardiac, intracarotid, and retro-orbital injection are advantageous. These techniques yield metastasis on a larger scale in a much shorter timeline than those involving a "primary" tumor. For studies of brain metastasis, in particular, models that reliably produce tumors in the brain parenchyma can be difficult to establish. In these cases, intracarotid and retro-orbital injection represent methods of bypassing organs with lower "barriers to entry," such as the liver and kidneys, which can cause premature mortality in mice injected via the intracardiac route.

The mouse genetic background of choice for xeno- or allograft transplantation depends on the source of cells (human, mouse) and, occasionally, on genetic modifications of the implanted cells that may elicit immune rejection. Experiments involving human xenograft models are usually conducted in mice with impaired adaptive and innate immune systems, NOD.Cg-*Prkdc*^{scid} *Il2rg*^{tm1Wjl}/SzJ (NSG) mice; or mice lacking adaptive immunity, such as T cell-deficient athymic/nude (NU/J) mice. Another immunodeficient model frequently used is the RAG2 knockout (KO) model, which lacks B and T cells and retains a functional natural killer cell population. These immunodeficient mouse models must be deployed strategically, as each has advantages at the expense of some drawbacks related to their intrinsic immune deficiencies. In the authors' experience, the same cell line- or patient-derived STCs exhibit different organ tropism based on the route of injection (e.g., subcutaneous vs. intracardiac) and/or the recipient mouse strain (e.g., NSG vs. athymic/nude) (see **Table 2**).

To mitigate the experimental variability pertaining to the host in which melanoma cells are implanted (e.g., immune response, microbiota), and maximize 'on target' and reproducible findings, the following are recommended: i) increasing the number of experimental animals per group (using power calculations to reach an optimal number based on the effect size), ii) using orthogonal methods to manipulate gene candidates (i.e., CRISPR/Cas9, CRISPRi, shRNA), and 'add-back' experiments (i.e., concomitant ectopic expression of a Cas9- or shRNA-resistant cDNA of the gene of interest). These complementary techniques reduce the impact of off-target effects and/or biological and experimental variation.

While this protocol can certainly be applied for hypothesis-driven validation of candidate drivers or suppressors of metastasis, these methods may also be useful for unbiased, exploratory studies. For example, pooled CRISPR/cas9, CRISPR-KRAB-dCas9 (CRISPRi), and shRNA-based screens allow for a process of Darwinian selection to play out *in vivo*[34]. The conceptual basis for such studies is as follows: a cell with a gene knocked out that is essential to the phenotype of interest (e.g., tumor growth) will die or fail to proliferate, such that its representation in the sequenced library is diminished at the conclusion of the experiment relative to the baseline. The procedures described here may be applied for such an approach, with appropriate optimization[35,36].

In regard to candidate gene selection, multiple sources can be mined. Melanoma patient transcriptomics and proteomics datasets are publicly available via the NCBI Gene Expression Omnibus (GEO)[37], the European Genome-Phenome Archive[38], cBioPortal[39] (which hosts The Cancer Genome Atlas, or TCGA[40]), and other hosting sites. Reanalysis of raw data is recommended as quality control measures can vary greatly between public databases, impacting the results. When interrogating raw datasets, questions appropriate for candidate gene selection suitable for application to the workflow described here include: which genes are dysregulated in metastatic samples as compared to primary melanoma samples or to melanocytic nevi?; which genes are dysregulated in specific sites of metastasis?; is the dysregulated expression of the candidate gene associated with improved patient survival?; is this gene part of a larger gene expression program that is generally dysregulated?; are the interactors of the gene product well-characterized or unknown?; is the gene product druggable, and if so, are targeting tools available?; and very importantly, is the gene essential to all human cells, or to many tissues, such that interference with its activity in a clinical setting might prove toxic?

The appropriate strategy for the manipulation of the genes of interest depends on the hypotheses to be tested. For example, a gene upregulated in metastasis can be knocked down to assess if the corresponding mice would display decreased metastatic burden compared to a control group. This approach is best carried out in a model cell line or short-term culture, which features both: a) high expression of the gene of interest and b) generates appreciable metastatic burden when injected into mice with reproducible kinetics. Knockdown approaches include shRNA- and CRISPR/Cas9 based-methods, both of which can be engineered via lentiviral infection of melanoma cells and deployed in an inducible or constitutive fashion. One of the advantages of inducible expression (see pLKO Tet-On in the **Table of Materials**) is the temporal regulation of knockdown, which can be leveraged in an *in vivo* experiment. Thus, inducible shRNAs/sgRNAs can be used to model a "therapeutic setting" in which established tumor cells are subjected to a candidate gene knockdown. However, exposure to the inducing agent, e.g., doxycycline, may have consequences for the behavior of certain melanoma cells; as such, the inclusion of control cells transduced with a scrambled shRNA that also experience this treatment is critical.

Whereas shRNAs often yield a partial knockdown of gene expression, CRISPR/Cas9-based systems edit a gene at the DNA level, theoretically eliciting a complete "knockout" (KO). Their use presents both advantages and disadvantages. If a gene is essential for melanoma cell viability,

cells with a complete KO will be negatively selected *in vitro* and later *in vivo*. Although this issue may be partially mitigated by selecting single-cell clones, melanoma cells struggle to grow from single cells, which results in unpredictable and often disparate adaptations. Thus, multiple KO clones need to be tested to control for interclonal phenotypic variations. Furthermore, in the case of patient-derived STCs especially, the number of lentiviral infections to which melanoma cells are exposed can greatly affect *in vitro* proliferation and *in vivo* metastatic behavior. Therefore, a single-vector, single-infection approach incorporating Cas9 and an sgRNA (see lentiCRISPRv2 in the **Table of Materials**) is recommended.

Other systems make use of a "recombinase dead" Cas9 to elicit transcriptional repression (dCas9-KRAB in the **Table of Materials**). A gain-of-function approach may be appropriate if a gene of interest is hypothesized to be a metastasis-promoting gene. In this case, the selection of a melanoma line yielding few metastases upon injection in mice and featuring low basal expression of the gene of interest is key. Overexpression constructs (particularly those driven by CMV promoters) often lead to supraphysiologic expression levels, which cause proteotoxic stress. Therefore, choosing lentiviral vectors that allow for the physiological expression of the gene of interest is recommended.

Once an approach has been selected, it is important to carry out the following experiments **prior to** the engraftment of cells. Lentiviral infection procedures vary between laboratories and will necessitate optimization for each cell line and knockdown system. However, universal considerations include a complete positive or negative selection of cells featuring gene knockdown (e.g., FACS/cell sorting for fluorescent reporters or antibiotic selection, if applicable), followed by RT-qPCR and western blot with appropriate controls to demonstrate reproducible and robust knockdown or overexpression of the gene of interest. An *in vitro* proliferation assay should be conducted to determine if interfering with the gene of interest affects cell viability. This step is important for reliable cell characterization and for the correct interpretation of *in vivo* results. Here is an example of a pitfall if the experiments described are not performed: if a gene knockdown results in a drastic proliferation defect *in vitro*, this will confound the interpretation of decreased metastatic burden, as the specific contribution of this gene to the metastatic cascade cannot be accurately assessed. Various modalities of proliferation assays include commercially available kits, live cell-imaging systems, or traditional cell-culture-based assays, e.g., crystal violet, trypan blue exclusion.

Among the major limitations for this platform in discovering mediators in melanoma is that the proposed workflow addresses only tumor cell-intrinsic gene candidates, not genes expressed by the cells of the surrounding microenvironment at different metastasis stages, which are key modulators of tumor cell adaptation and seeding of distal organs. Another important factor to consider is differential metastatic behavior based on the engraftment route. The interlaboratory and interoperator variability intrinsic to some of the techniques presented can be addressed by standardization across the metastasis research field. Currently, the most suitable protocol for standardization is the intracardiac injection due to the ultrasound guidance and static injection devices, which remove interoperator variability. This protocol represents one of the numerous steps in the direction of uniformity, reproducibility, and thorough documentation of methods

used across laboratories working on the identification of novel mediators of melanoma metastasis.

ACKNOWLEDGMENTS:

We thank the Division of Advanced Research Technologies (DART) at NYU Langone Health, and in particular, the Experimental Pathology Research Laboratory, Genome Technology Center, Cytometry and Cell Sorting Laboratory, Pre-Clinical Imaging Core, which are partially supported by the Perlmutter Cancer Center Support Grant NIH/NCI 5P30CA016087. We thank the NYU Interdisciplinary Melanoma Cooperative Group (PI: Dr. Iman Osman) for providing access to patient-derived melanoma short-term cultures (10-230BM and 12-273BM), which were obtained through IRB-approved protocols (Universal Consent study #s16-00122 and Interdisciplinary Melanoma Cooperative Group study #10362). We thank Dr. Robert Kerbel (University of Toronto) for providing 113/6-4L and 131/4-5B1 melanoma cell lines and Dr. Meenhard Herlyn (Wistar Institute) for providing WM 4265-2, WM 4257s-1, WM 4257-2 melanoma short-term cultures. E.H. is supported by NIH/NCI R01CA243446, P01CA206980, an American Cancer Society-Melanoma Research Alliance Team Science Award, and an NIH Melanoma SPORE (NCI P50 CA225450; PI: I.O.). **Figure 1** was created with Biorender.com.

DISCLOSURES:

The authors have no conflicts of interest to declare.

REFERENCES:

1. Sung, H. et al. Global Cancer Statistics 2020: GLOBOCAN Estimates of incidence and mortality worldwide for 36 cancers in 185 countries. *CA: A Cancer Journal for Clinicians*. **71** (3), 209–249 (2021).
2. Adler, N. R., Haydon, A., McLean, C. A., Kelly, J. W., Mar, V. J. Metastatic pathways in patients with cutaneous melanoma. *Pigment Cell Melanoma Research*. **30** (1), 13–27 (2017).
3. Platz, A., Egyhazi, S., Ringborg, U., Hansson, J. Human cutaneous melanoma; a review of NRAS and BRAF mutation frequencies in relation to histogenetic subclass and body site. *Molecular Oncology*. **1** (4), 395–405 (2008).
4. Alonso, S. R. et al. A high-throughput study in melanoma identifies epithelial-mesenchymal transition as a major determinant of metastasis. *Cancer Research*. **67** (7), 3450–3460 (2007).
5. Rowe, C. J., Khosrotehrani, K. Clinical and biological determinants of melanoma progression: Should all be considered for clinical management? *Australasian Journal of Dermatology*. **57** (3), 175–181 (2016).
6. Plebanek, M. P. et al. Pre-metastatic cancer exosomes induce immune surveillance by patrolling monocytes at the metastatic niche. *Nature Communications*. **8** (1), 1319 (2017).
7. Orgaz, J. L. et al. Loss of pigment epithelium-derived factor enables migration, invasion and metastatic spread of human melanoma. *Oncogene*. **28** (47), 4147–4161 (2009).
8. Ladhani, O., Sanchez-Martinez, C., Orgaz, J. L., Jimenez, B., Volpert, O. V. Pigment epithelium-derived factor blocks tumor extravasation by suppressing amoeboid morphology and mesenchymal proteolysis. *Neoplasia*. **13** (7), 633–642 (2011).

9. Ju, R. J., Stehbens, S. J., Haass, N. K. The role of melanoma cell-stroma interaction in cell motility, invasion, and metastasis. *Frontires in Medicine - Dermatology*. **5**, 307 (2018).
10. Wiley, H. E., Gonzalez, E. B., Maki, W., Wu, M. T., Hwang, S. T. Expression of CC chemokine receptor-7 and regional lymph node metastasis of B16 murine melanoma. *Journal of the National Cancer Institute.* **93** (21), 1638–1643 (2001).
11. Meier, F. et al. Metastatic pathways and time courses in the orderly progression of cutaneous melanoma. *British Journal of Dermatology*. **147** (1), 62–70 (2002).
12. Turner, N., Ware, O.,Bosenberg, M. Genetics of metastasis: melanoma and other cancers. *Clinical & Experimental Metastasis*. **35** (5–6), 379–391 (2018).
13. Ubellacker, J. M. et al. Lymph protects metastasizing melanoma cells from ferroptosis. *Nature*. **585** (7823), 113–118 (2020).
14. Cukierman, E., Pankov, R., Stevens, D. R., Yamada, K. M. Taking cell-matrix adhesions to the third dimension. *Science*. **294** (5547), 1708–1712 (2001).
15. Cunningham, C. C. et al. Actin-binding protein requirement for cortical stability and efficient locomotion. *Science*. **255** (5042), 325–327 (1992).
16. Unger, C. et al. Modeling human carcinomas: physiologically relevant 3D models to improve anti-cancer drug development. *Advanced Drug Delivery Reviews*. **79**–**80**, 50–67 (2014).
17. Fong, E. L., Harrington, D. A., Farach-Carson, M. C., Yu, H. Heralding a new paradigm in 3D tumor modeling. *Biomaterials*. **108**, 197–213 (2016).
18. Nakamura, K. et al. Characterization of mouse melanoma cell lines by their mortal malignancy using an experimental metastatic model. *Life Science*. **70** (7), 791–798 (2002).
19. Meeth, K., Wang, J. X., Micevic, G., Damsky, W., Bosenberg, M. W. The YUMM lines: a series of congenic mouse melanoma cell lines with defined genetic alterations. *Pigment Cell Melanoma Research*. **29** (5), 590–597 (2016).
20. Koya, R. C. et al. BRAF inhibitor vemurafenib improves the antitumor activity of adoptive cell immunotherapy. *Cancer Research*. **72** (16), 3928–3937 (2012).
21. Jenkins, M. H. Multiple murine BRaf(V600E) melanoma cell lines with sensitivity to PLX4032. *Pigment Cell Melanoma Research*. **27** (3), 495–501 (2014).
22. Tuncer, E. et al. SMAD signaling promotes melanoma metastasis independently of phenotype switching. *The Journal of Clinical Investigation*. **129** (7), 2702–2716 (2019).
23. Schwartz, H. et al. Incipient Melanoma Brain Metastases Instigate Astrogliosis and Neuroinflammation. *Cancer Research*. **76** (15), 4359–4371 (2016).
24. Perez-Guijarro, E. et al. Multimodel preclinical platform predicts clinical response of melanoma to immunotherapy. *Nature Medicine*. **26** (5), 781–791 (2020).
25. Krepler, C. et al. A Comprehensive Patient-Derived Xenograft Collection Representing the Heterogeneity of Melanoma. *Cell Reports*. **21** (7), 1953–1967 (2017).
26. Agrawal, P. et al. A systems biology approach identifies FUT8 as a driver of melanoma metastasis. *Cancer Cell*. **31** (6), 804–819.e7 (2017).
27. Hanniford, D. et al. Epigenetic silencing of CDR1as drives IGF2BP3-mediated melanoma invasion and metastasis. *Cancer Cell*. **37** (1), 55–70.e15 (2020).
28. Kim, H. et al. PRMT5 control of cGAS/STING and NLRC5 pathways defines melanoma response to antitumor immunity. *Science Translational Medicine*. **12** (551), eaaz5683 (2020).

29. de Miera, E. V., Friedman, E. B., Greenwald, H. S., Perle, M. A., Osman, I. Development of five new melanoma low passage cell lines representing the clinical and genetic profile of their tumors of origin. *Pigment Cell Melanoma Re*search. **25** (3), 395–397 (2012).
30. Morsi, A., et al. Development and characterization of a clinically relevant mouse model of melanoma brain metastasis. *Pigment Cell Melanoma Research*. **26** (5), 743–745 (2013).
31. Zou, C. et al. Experimental variables that affect human hepatocyte AAV transduction in liver chimeric mice. *Molecular Therapy Methods and Clinical Development*. **18**, 189–198 (2020).
32. Curtis, A., Calabro, K., Galarneau, J. R., Bigio, I. J. Krucker, T. Temporal variations of skin pigmentation in C57BL/6 mice affect optical bioluminescence quantitation. *Molecular Imaging and Biology*. **13** (6), 1114–1123 (2011).
33. Sil, P., Wong, S. W., Martinez, J. More than skin deep: autophagy is vital for skin barrier function. *Frontiers in Immunology*. **9**, 1376 (2018).
34. Chen, S. et al. Genome-wide CRISPR screen in a mouse model of tumor growth and metastasis. *Cell*. **160** (6), 1246–1260 (2015).
35. Hart, T. et al. High-resolution CRISPR screens reveal fitness genes and genotype-specific cancer liabilities. *Cell*. **163** (6), 1515–1526 (2015).
36. Wang, T. et al. Identification and characterization of essential genes in the human genome. *Science*. **350** (6264), 1096–1101 (2015).
37. Edgar, R., Domrachev, M., Lash, A. E. Gene Expression Omnibus: NCBI gene expression and hybridization array data repository. *Nucleic Acids Research*. **30** (1), 207–210 (2002).
38. Lappalainen, I., et al. The European Genome-phenome Archive of human data consented for biomedical research. *Nature Genetics*. **47** (7), 692–695 (2015).
39. Cerami, E. et al. The cBio cancer genomics portal: an open platform for exploring multidimensional cancer genomics data. *Cancer Discovery.* **2** (5), 401–404 (2012).
40. Grossman, R. L., et al. Toward a shared vision for cancer genomic data. *New England Journal of Medicine*. **375** (12), 1109–1112 (2016).

Figure 1

Click here to access/download;Figure;Figure 1 Final (1).pdf

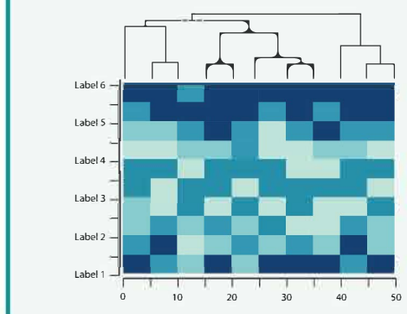

Integration of patient datasets

Candidate gene selection

LOF/GOF model systems

Lentiviral transduction
Proliferation assay
Western blot

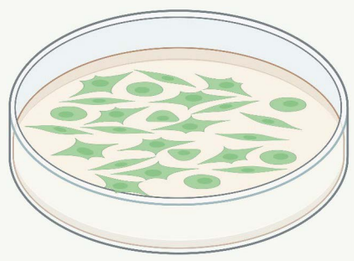

In vivo functional experiments

Subcutaneous
Intradermal
Intracardiac

Omics

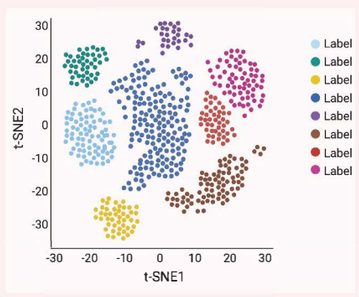

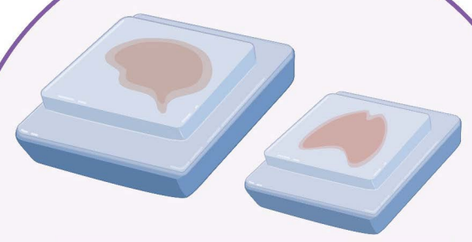

Histopathology

Immuno-fluorescence

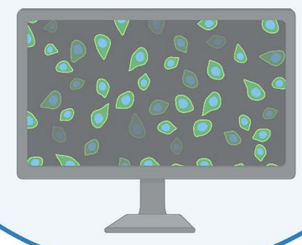

Figure 2

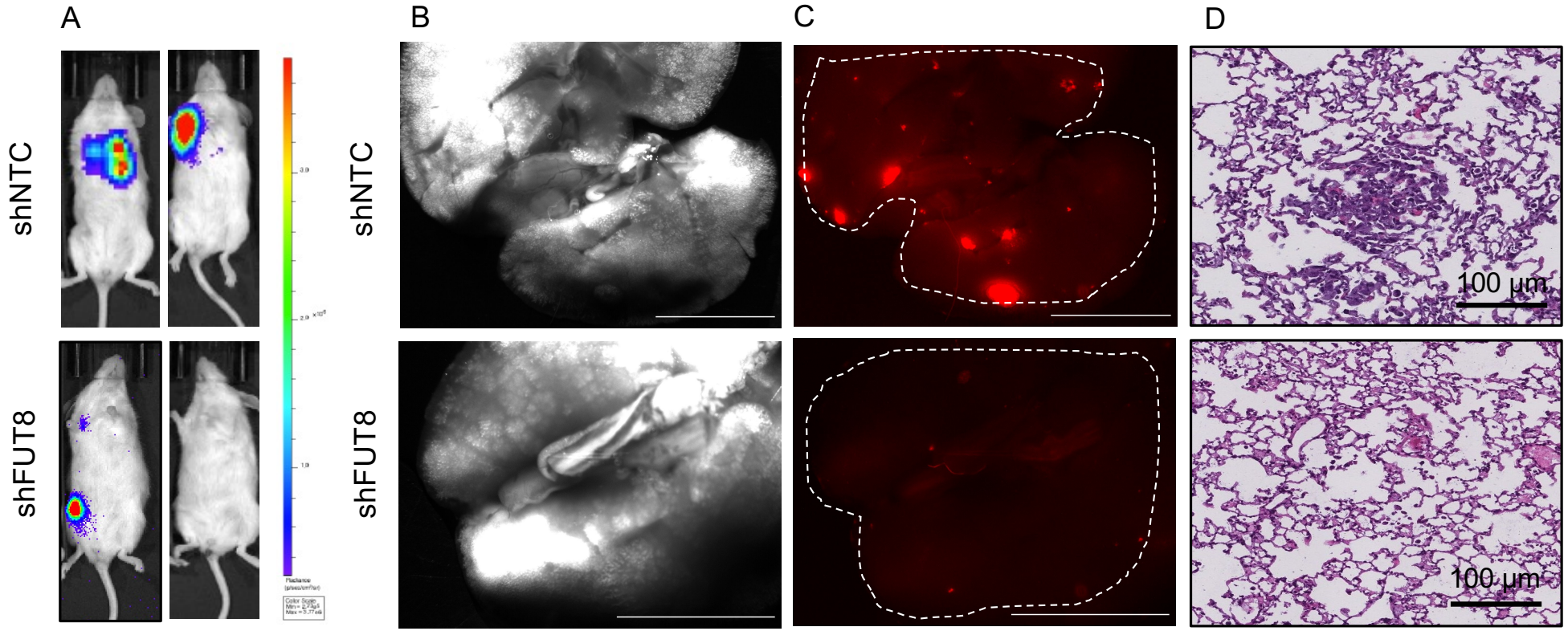

Figure 3

Click here to access/download;Figure;Figure 3 Final - visiopharm_cropped.pdf

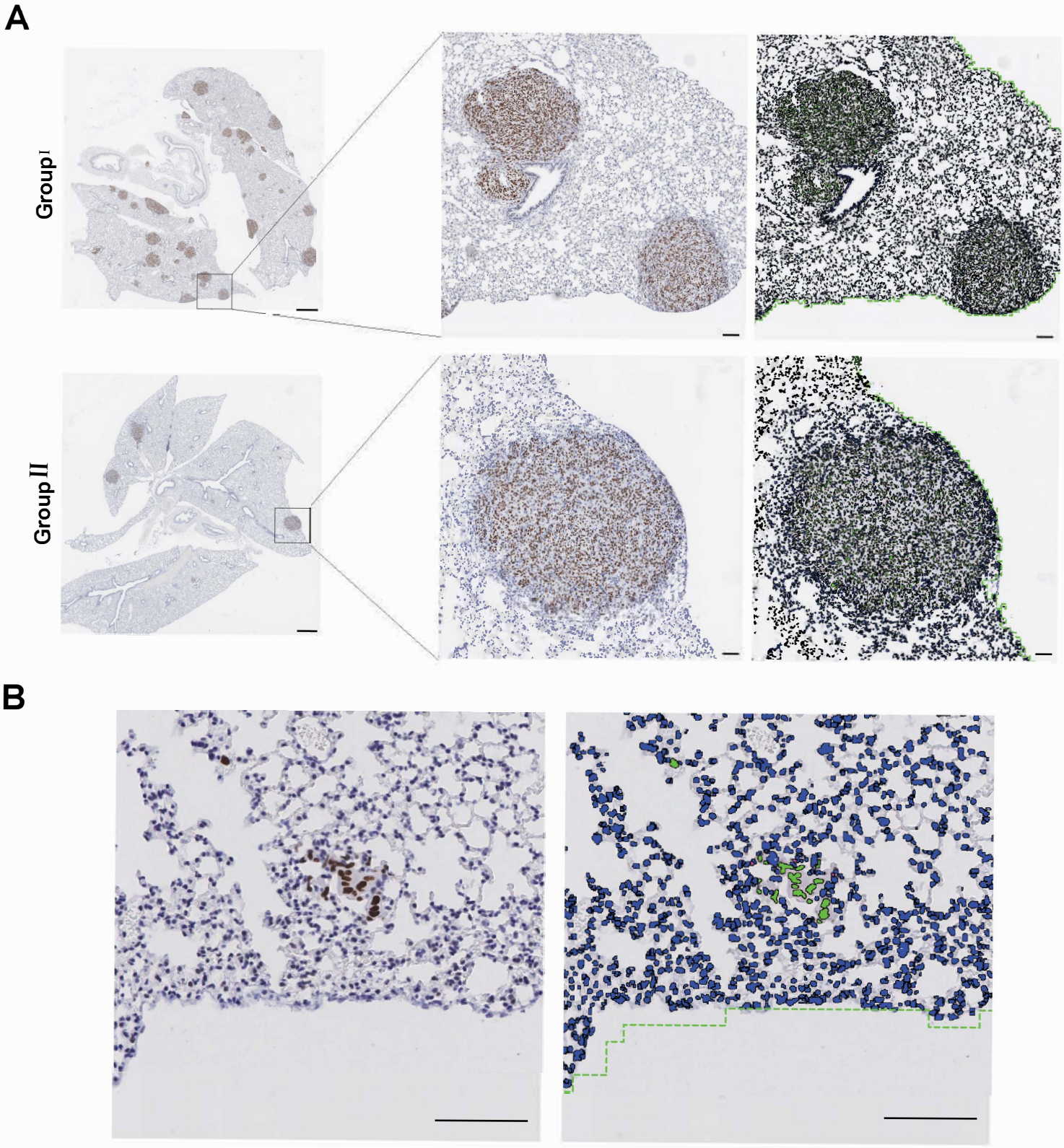

Table 1

Antibody	Manufacturer	Catalog No	Host species	Reactivity	Fluorophore	Dilution	Incubation time (h)	Incubation temperature
anti-GFP	Abcam	ab6556	Rabbit	Mouse	unconjugate	1:1,000	24	4 ℃
anti-GFAP	Aves Labs	GFAP	Chicken	Mouse	unconjugate	1:2,000	24	4 ℃
secondary	Invitrogen	a11041	Goat	Chicken	A568	1:500	2	Room Temperature
secondary	Invitrogen	a32731	Goat	Rabbit	A488	1:500	2	Room Temperature

Table 2

Cell Line	Type	Time to euthanasia	Sex of Mice	Genetic Background of Mice	Route of injection	# Cells Injected	Sites of metastasis
12-273 BM^{+}	Human melanoma STC	4-5 weeks	M	NSG	Intracardiac	100K	Brain parenchyma, leptomeninges, liver, kidney, adrenal glands
131/4-5B1*	Human melanoma	4 weeks	M	Athymic nude	Intracardiac	100K	Brain parenchyma, liver, lung
113/6-4L*	Human melanoma	5 weeks	F	Athymic nude	Intracardiac	50K	Brain parenchyma (few), liver, lung
WM 4265-2**	Human melanoma STC	11 weeks	M	NSG/athymic nude	Intracardiac	200K	Brain parenchyma
WM 4257-1**	Human melanoma STC	10-13 weeks	M	Athymic nude	Intracardiac	100K	Brain parenchyma
WM 4257-2**	Human melanoma STC	10-13 weeks	M	Athymic nude	Intracardiac	100K	Brain parenchyma
10-230 BM^{+}	Human melanoma STC	8-9 weeks	M	Athymic nude	Intracardiac	100K	Brain parenchyma, leptomeninges, liver, kidney, adrenal glands

Dear Dr. Vidhya Iyer,

We thank you and the reviewers for your thorough assessment of the manuscript. In this revised version of our manuscript, we have addressed all the comments and suggestions and tracked the changes made as indicated. We added 1 new Table with the immunofluorescence conditions and antibodies used and revised Figure 2 in order to increase the ease of reading as you suggested.

Thank you for your time and consideration,

Respectfully yours,
Arman Alberto Sorin Shadaloey,
Research Scientist.